Low-lying intruder and tensor-driven structures in ^{82}As revealed by β decay at a new movable-tape-based experimental setup

A. Etilé,[1] D. Verney,[2] N. N. Arsenyev,[3] J. Bettane,[2] I. N. Borzov,[3,4] M. Cheikh Mhamed,[2] P. V. Cuong,[5] C. Delafosse,[2] F. Didierjean,[6] C. Gaulard,[1] Nguyen Van Giai,[2] A. Goasduff,[1] F. Ibrahim,[2] K. Kolos,[2,*] C. Lau,[2] M. Niikura,[2,†] S. Roccia,[1] A. P. Severyukhin,[3] D. Testov,[2,7] S. Tusseau-Nenez,[2] and V. V. Voronov[3]

[1]*CSNSM, CNRS/IN2P3 and Université Paris Sud, Orsay, France*
[2]*Institut de Physique Nucléaire, CNRS/IN2P3 and Université Paris Sud, Orsay, France*
[3]*Bogoliubov Laboratory of Theoretical Physics, Joint Institute for Nuclear Research, Dubna, Russia*
[4]*National Research Center "Kurchatov Institute", Moscow, Russia*
[5]*Center for Nuclear Physics, Institute of Physics, Vietnam Academy of Science and Technology, Hanoi, Vietnam*
[6]*Institut Pluridisciplinaire Hubert Curien, CNRS/IN2P3 and Université de Strasbourg, Strasbourg, France*
[7]*Flerov Laboratory of Nuclear Reactions, Joint Institute for Nuclear Research, Dubna, Russia*

(Received 5 February 2015; published 26 June 2015)

The β decay of ^{82}Ge was re-investigated using the newly commissioned tape station BEDO at the electron-driven ISOL (isotope separation on line) facility ALTO operated by the Institut de Physique Nucléaire, Orsay. The original motivation of this work was focused on the sudden occurrence in the light $N = 49$ odd-odd isotonic chain of a large number of $J \leqslant 1$ states (positive or negative parity) in ^{80}Ga by providing a reliable intermediate example, viz., ^{82}As. The extension of the ^{82}As level scheme towards higher energies from the present work has revealed three potential 1^+ states above the already known one at 1092 keV. In addition our data allow ruling out the hypothesis that the 843 keV level could be a 1^+ state. A detailed analysis of the level scheme using both an empirical core-particle coupling model and a fully microscopic treatment within a Skyrme-QRPA (quasiparticle random-phase approximation) approach using the finite-rank separable approximation was performed. From this analysis two conclusions can be drawn: (i) the presence of a large number of low-lying low-spin negative parity states is due to intruder states stemming from above the $N = 50$ shell closure, and (ii) the sudden increase, from ^{82}As to ^{80}Ga, of the number of low-lying 1^+ states and the corresponding Gamow-Teller fragmentation are naturally reproduced by the inclusion of tensor correlations and couplings to 2p-2h excitations.

DOI: 10.1103/PhysRevC.91.064317 PACS number(s): 23.40.−s, 27.50.+e, 29.25.Rm, 21.60.Jz

I. INTRODUCTION

The $N = 49$ isotonic line, from stability towards ^{77}Ni, provides a wealth of intriguing structure phenomena, the first of which being the relative evolutions of normal one-hole (1h) and very low lying (positive parity) one-particle, two-hole (1p-2h) intruder states in the $N = 49$ odd isotones, originally noticed some three decades ago by Hoff and Fogelberg in their seminal work of Ref. [1]. From $^{83}_{34}$Se$_{49}$ to $^{81}_{32}$Ge$_{49}$ the nature of the first excited (and isomeric) state changes for the first time, switching from $1/2^-$ to $1/2^+$; that is, supposedly from a $\nu 2p^{-1}_{1/2}$ to a $\nu(1g^{-2}_{9/2}3s^1_{1/2})$ nature [1]. Consistent systematics of these 1h and 1p-2h states have been proposed in Refs. [1,2] (see Fig. 10 in Ref. [1] and Fig. 2 in Ref. [2]; see also Fig. 3.25 in Ref. [3]). In Ref. [2], the energy minimum found at $Z = 34$ for the intruder states was ascribed to a natural mid proton (28-40) shell effect[1] in analogy to similar behavior of intruder states observed along the $Z = 49$ line. However the significantly steeper increase of the energy of the $\nu 2p^{-1}_{1/2}$ state from $Z = 34$ to 32 has not yet found any satisfactory explanation (actually no explanation at all, to our knowledge). In general the problem of the intruder configurations in the region $N \approx 50, Z < 40$, has not been addressed experimentally for more than three decades, as pointed out in the recent review on the subject [4].

The second intriguing phenomenon in this mass region is the considerable amount of very low spin states populated in β decay which seem to appear suddenly for $^{80}_{31}$Ga$_{49}$ in the sequence of the light odd-odd $N = 49$ isotones. The study of the β decay of ^{80}Zn had attracted considerable interest as soon as it became available as a beam at early ISOL (isotope separator on line) facilities such as OSIRIS or TRISTAN, because this nucleus was considered to be an r-process waiting point [5–7] and has been re-investigated very recently [8]. It is useful to recall that it is in trying to theoretically account for the observed number of states populated in ^{80}Ga from the decay of ^{80}Zn (using a random-phase approximation model) that Kratz *et al.* first introduced the concept of "a rapid weakening of the shell strength far from β stability above ^{78}Ni" [9]. It was indeed only by employing a quadrupole deformation parameter ϵ_2 of 0.26—a considerable value for a nucleus situated next to a closed shell—that 1^+ states could appear in the level scheme of ^{80}Ga as low as ≈600 keV (it was visibly assumed in Ref. [9], though not clearly stated, that a 1^+ assignment was made to *all* the experimental levels). The knowledge of spectral distribution of the 1^+ states in odd-odd nuclei and the

[*]Present address: University of Tennessee, Knoxville, Tennessee 37996, USA.

[†]Present address: Department of Physics, University of Tokyo, Hongo, Bunkyo-ku, Tokyo 113-0033, Japan.

[1]More precisely, it was ascribed to an effect of the proton subshell at $Z = 40$ in suppressing the normal occurrence of intruder states at minimal energy at mid proton (28–50) shell.

understanding of their structure are of primary importance as these two features determinate the half-life of the decaying even-even mother nuclei.

It is from the above considerations, and in particular, noting the large difference in number of observed low-spin states between ^{82}As and ^{80}Ga, that one may wonder if an important structure effect is at play along the $N = 49$ line from stable to proton-deficient nuclei. ^{82}As constitutes an interesting intermediate case that should hold the fingerprints of these supposed evolutions. By the course of the preparation of this article new data on the ^{82}Ge decay were released by the Oak Ridge group [10]. However, when we chose to undertake this study, spectroscopic information on ^{82}As was still scarce. Population of excited levels of ^{82}As has indeed been reported only twice before the year 2014: in the ^{82}Se(t, ^{3}He) reaction [11] and in the β decay of ^{82}Ge [1]. We felt that re-investigation of the structure of ^{82}As via β-decay spectroscopy at ALTO could be in order.

We have seized the opportunity of a test run at the ALTO ISOL facility dedicated to the commissioning of the new movable tape based β-decay experimental setup BEDO (BEta Decay studies at Orsay) for that purpose. Because the present paper reports on the first β-decay results ever obtained at the on-line mass separator PARRNe with a setup different from the "historical" one used so far, the BEDO setup will be briefly introduced in Sec. II. A new level scheme for ^{82}As will be proposed in Sec. III and the structure of this nucleus discussed in Sec. IV in relation with the questions mentioned above.

II. EXPERIMENTAL ARRANGEMENT

A. ^{82}Ge source preparation

^{82}Ge nuclei were obtained as mass separated fission fragments at the PARRNe mass separator operating on line at the electron-driven ALTO ISOL installation of the Institut de Physique Nucléaire, Orsay [12,13]. A target of 63 g of ^{238}U in the form of 85 UC_x pellets ($\approx$13.5 mm diameter, 1 mm thickness), with about 1 weight percent of graphite in excess, arranged into a graphite container placed into a Ta oven heated up to $\geqslant$2000 °C was exposed to the primary 50 MeV electron beam delivered by the ALTO linear accelerator. The average electron beam current on the target was $\simeq$7 μA. For this BEDO commissioning run, the oven was connected to a homemade, hot plasma ion source which was chosen for its poor elemental selectivity because we wanted to test the selectivity of the detection setup in the most penalizing situation of mixed sources.

The PARRNe mass-separator magnetic field was set for selection of 1^+ charge state ions with mass number 82. The sources were constituted by the interception of the 30 keV $A = 82$ radioactive ion beam by an Al-coated Mylar movable tape at the exact geometrical center of the BEDO detector assembly. In order to enhance shorter lived activities the tape was moved every 4 s after a 2 s build-in followed by a 2 s decay time. The $A/Q = 82$ beam was essentially dominated by the activity from ^{82}Ga and quite unexpectedly by that of ^{132}Sn. No evidence was found for activities shorter than the period of ^{82}Ga ($T_{1/2} = 599 \pm 2$ ms [14]). The time spectrum of the

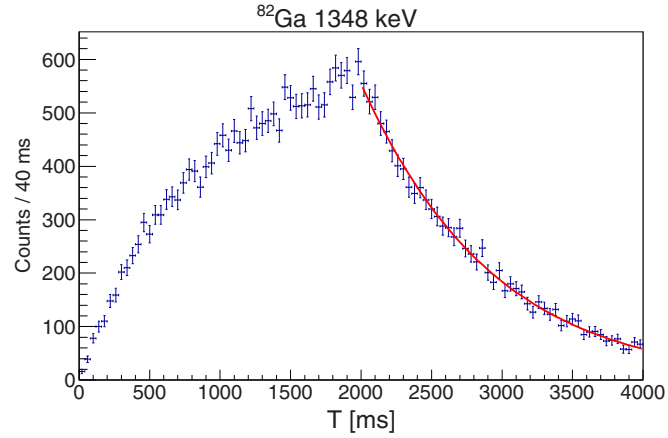

FIG. 1. (Color online) Time evolution of the 1348 keV line from the ^{82}Ga activity. The fit of the decay part of the curve gives $T_{1/2} = 592 \pm 9$ ms (in good agreement with the adopted value $T_{1/2} = 599 \pm 2$ ms [14]).

1348 keV γ line from the ^{82}Ga activity (transition $2_1^+ \rightarrow 0_{gs}^+$ in ^{82}Ge) is shown in Fig. 1 as a typical example.

As already mentioned we discovered that our γ spectra were significantly contaminated by an activity from ^{132}Sn (see Fig. 5 in Sec III). Systematic yield evaluations using the observed γ intensities, tabulated branching ratios, and after correction for cycle efficiencies are reported in Table I. We must conclude that activities from heavy Sn and Sb isotopes at $A/Q = 82$ originate from the presence of molecular components in the beam, of the type XS^{2+} or XO_2^{2+}. The fact that we did not detect any activity from ^{131}Sn decay favors the hypothesis of sulfide ions. In addition, crystallogens such as Sn are well known to easily form sulfide molecules in ISOL conditions, a property apparently relatively independent from the form and choice of the sulfide-forming agent; see [15,16] and Refs. therein. It is possible then that the presence of S in the form of traces in some component of the target-ion-source system has been sufficient to lead to the formation of SnS molecules. However, to our knowledge, observation of multiple charged sulfide ions has never been reported before. The question will deserve further investigation as such serendipity may help in considering alternatives for the production at ALTO of beams of heavy Sn isotopes at mass-separator $B\rho$ values where their usual strong isobaric contaminants could be absent. As seen in Table I, we note also the possible presence of Sb in molecular form in the beam. In

TABLE I. Beam composition as observed in this experiment.

Nucleus	Yield (pps)	A/Q	Note
^{82}Ga	$\approx 3 \times 10^2$	82/1	atomic
^{82}Ge	$\approx 7 \times 10^2$	82/1	atomic
^{132}Sn	$\approx 2.8 \times 10^3$	164/2	$(^{132}Sn^{32}S)^{2+}$
^{130}Sn	$\approx 9 \times 10^2$	164/2	$(^{130}Sn^{34}S)^{2+}$
^{132}Sb	$\approx 2.7 \times 10^3$	164/2	molecular: ?
^{130}Sb		164/2	possible traces

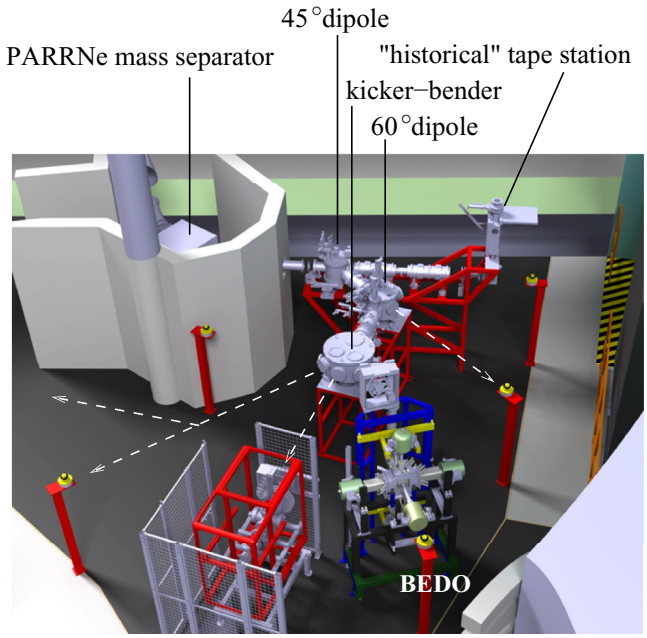

FIG. 2. (Color online) Location of BEDO after the new secondary beam lines in the mass-separator room (hall 110) of the ALTO facility. Other possible future beam lines are represented by white doted lines.

principle, the formation of Sb sulfides is not favored [15,16]. However the numbers for Sb in Table I are to be taken with caution: ^{130,132}Sb have very long half-lives with respect to the tape cycle periods and the decay chains are complicated by the presence of isomers. In addition the activity of ^{130}Sb was only revealed by very small peaks in the spectra.

B. Detection setup: BEDO

1. The BEDO concept

For a decade or so, β-decay spectroscopy experiments (our previous works from [17] to [18] and Refs. therein) have been performed at the "historical" tape station (see Fig. 2). It was originally built for identification and yield measurements only and could not accommodate more than two small Ge detectors. The opportunity to build a more complex detection system was offered by the completion of a new set of secondary beam line sections within the ALTO project; see Fig. 2 (to be compared to Fig. 2 in Ref. [19], for instance). To enter this new set, the beam is deviated at the approximate mass-separator focal plane by a 45° electrostatic dipole, then directed towards a three-branch kicker-bender *via* a second, 60° electrostatic dipole. The new movable tape collector was installed after the left arm of the kicker-bender. These two subsequent deviations, $45° + 60°$, were made necessary by the cake-like shape of the hall of the former Tandem line 110, to maximize as much as possible the number of potential sites for semi permanent installations of detection setups (six in total, including the "historical" tape station, see Fig. 2).

The trajectory of the tape in BEDO was chosen to maximize the space available around the beam collection point, ideally 4π, allowing the closest positioning of different types of detectors and maximal efficiency. The mechanical support was also designed to host various detector assemblies (from small scintillators [20] to a 4π ^{3}He long-counter [21,22]).

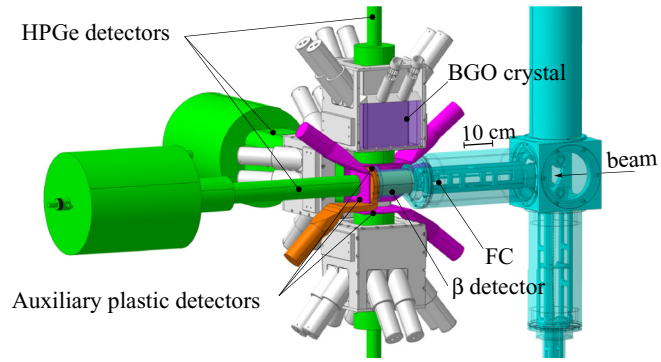

FIG. 3. (Color online) A schematic view of the BEDO detector assembly. FC stands for (retractable) Faraday cup.

For this test run we used the decay spectroscopy configuration as shown in Fig. 3. In this geometry the arrangement consists, *in principle* (as it was originally designed to be), of the four small EXOGAM clover detectors from the prototype series, positioned in cross geometry in the plan orthogonal to the beam axis which intercepts this axis at the collection point, plus a fifth position in the beam axis for a Ge detector of another type. The closest point of approach between end cap and collection point is ≈50 mm. In order to maximize the selectivity, a set of homemade auxiliary and guard detectors are added:

(i) The collection point is surrounded by a 3 mm thick, 98 mm long, 51 mm diameter cylindrical plastic (BC408) scintillator for the β trigger.
(ii) Four guard detectors were designed to fit the small EXOGAM clovers' geometry: each unit is composed of four independent $100 \times 130 \times 20$ mm^3 BGO (bismuth germanate) crystals wrapped into teflon, each of the crystals being optically connected to two 1″ photomultiplier tubes (Hamamatsu R7899-01).
(iii) Five plastic scintillators, made of a 3 mm thick BC408 rectangle wrapped into a 30 μm thick Al foil are positioned in front of each of the five Ge detector end caps. They can be used for Bremsstrahlung vetoing.

2. BEDO configuration for the commissioning experiment

However, by the time of this commissioning run, among these auxiliary detectors, only the β detector and one of the BGO shields were installed or operational. In addition, two of the small EXOGAM clover prototypes were replaced by coaxial detectors. The actual temporary Ge configuration for the present experiment then included

(i) two EXOGAM prototypes, with a resolution of 2.4 keV at 1 MeV;
(ii) two tapered Ge detector of the EUROGAM-1 type, 2.6 keV at 1 MeV;

(iii) one large volume coaxial Ge detector, 2.7 keV at 1 MeV.

This offered a global efficiency of 3.7% at 1 MeV. The efficiency of the $4\pi\beta$ detector was measured to be ≈55% with no energy dependence. The detector positioned in the BGO shield was a tapered Ge detector of the EUROGAM-1 type. The global performance of the system in nominal (four clovers, all auxiliary detectors active) configuration will be given in a forthcoming paper, however we will comment here the effect of the active shielding on β-gated γ spectra in the specific context of build-up followed by decay of cyclically evacuated mixed sources in ISOL conditions (as the subject has been unfortunately only rarely covered) in the BEDO geometry.

3. *BGO guard detectors for Compton suppression*

The use of active shielding becomes of primary importance for the detection of very weak activities onto the tape in a relatively hostile γ environment. As can be seen on Fig. 2 the mass separator is not far from the detection setup and we have observed in the past (e.g., Fig. 1 in Ref. [23]) strong activities from the region of the focal plane (located between the mass separator shielding wall and the 45° dipole). Although the BGO guard detectors were originally meant for shielding purposes only, opportunity was taken to assess their usefulness in Compton suppression mode.

It is commonly admitted that Compton suppression is of secondary importance in β-delayed γ spectroscopy, probably because sensitivity concepts emanating from high-spin physics are generally, erroneously, directly imported. As can be seen in Fig. 4, though not optimized for it, these simple shields seem to also provide an interesting, non-negligible contribution to the background reduction when used for Compton rejection. In the lower panel of Fig. 4 is reported the average background level reduction $BS = 1 - \bar{B}_S/\bar{B}_U$ ($\bar{B}_S$ and $\bar{B}_U$: the average background levels in the suppressed and unsuppressed spectra respectively—all quantities with subscript S and U have the same meaning in the following): around 40% of the background is rejected in the expected region of efficiency. But to qualitatively assess the impact of Compton rejection on the specific case of build-up followed by decay of cyclically evacuated mixed sources, one should rather rely on more adequate quantities derived from the notion of detection limit, like the minimum detectable activity (MDA).

The detection limit is by definition [24] the number of counts above which detection is certain within a given confidence limit. One can conveniently use the working expression given in Table 2 of Ref. [24] for the "well known blank," which applies for peak evaluations [25]. The detection limit (95% confidence limit) then reads

$$L_D = 2.71 + 3.29\sigma_0 \text{ counts},$$

where σ_0 is the standard deviation of the count distribution for a mean net count equal to zero above the background. In practice we had $\sigma_0 \approx \sqrt{2B}$, where B is the estimate of background beneath the peak. Following [24] one can define a MDA, a_D, as

$$L_D = K\, a_D.$$

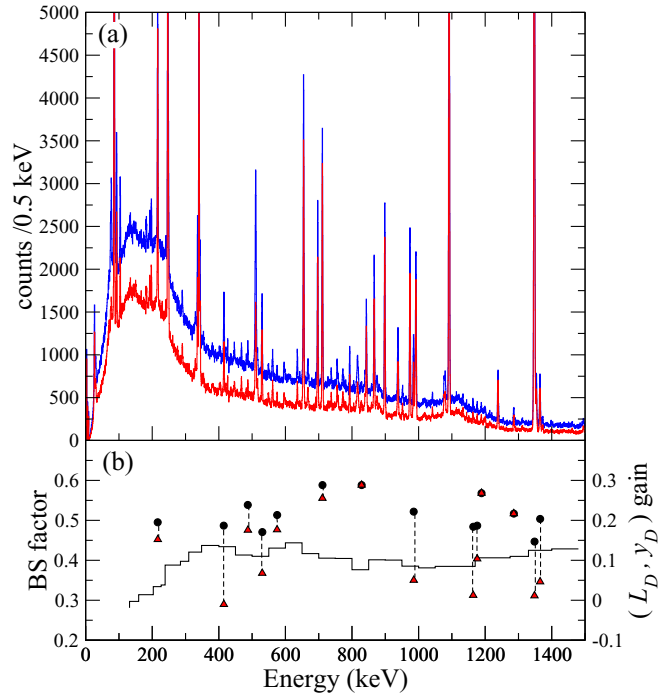

FIG. 4. (Color online) Upper panel (a): β-gated γ spectrum obtained at $A/Q = 82$ in this experiment with a tapered Ge detector of type EUROGAM-1 surrounded by one of the BEDO BGO shields. The total spectrum and Compton-suppressed spectrum are in blue an red respectively. Lower panel (b): The segmented line represents the average background suppression factor (left vertical scale), black circles and red triangles represent the gain in detection limit (L_D) and gain in minimum detectable yield (y_D), respectively (right vertical scale). See text for all definitions.

However, in the particular ISOL context, one is usually interested in the smallest production yields of the shortest lived nuclei in presence of larger long-lived activities from the beam and/or from decay daughters. In general the half-lives of the shortest lived activities reachable ($\lesssim$300 ms) would be small compared to the counting period, so that in first approximation one can consider saturation with the beam of the activity of the most interesting species onto the tape. Hence, one may consider an alternative, approximate quantity, a *minimum detectable yield* (MDY), y_D:

$$L_D \propto K\, y_D$$

with

$$K = \epsilon \times P_\gamma,$$

where ϵ is the full-energy peak efficiency and P_γ the emission probability of the gamma per decay.

The gain in detection limit $1 - L_{DS}/L_{DU}$ was evaluated for the peaks corresponding to the shortest observed activity, in our case ^{82}Ga decay, and the corresponding values are represented by black dots in the lower panel of Fig. 4. This gain is the maximum achievable gain in MDY since

$$\frac{y_{DS}}{y_{DU}} = \frac{L_{DS}}{L_{DU}} \times \frac{\epsilon_U}{\epsilon_S},$$

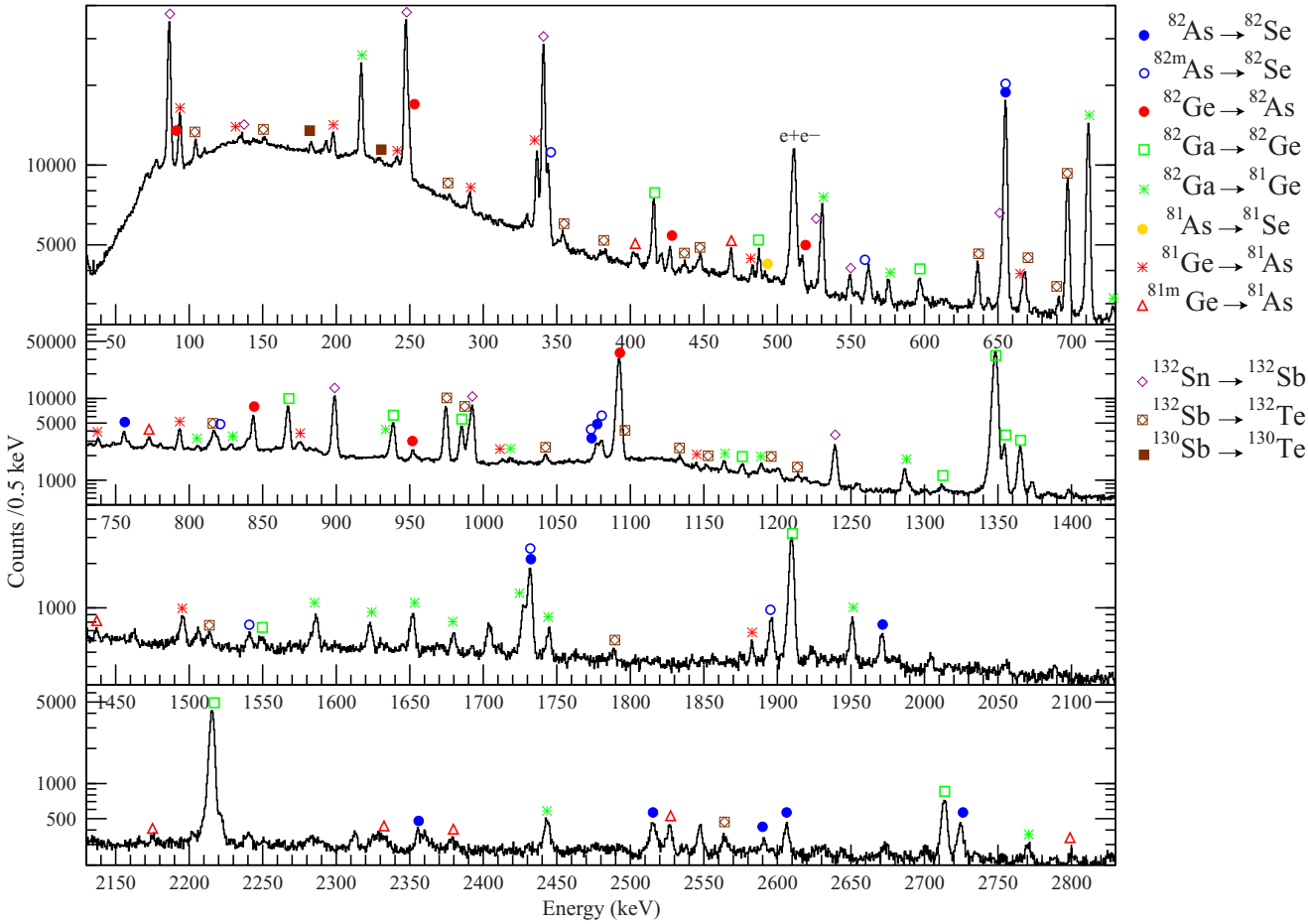

FIG. 5. (Color online) Experimental β-gated γ spectrum obtained at $A/Q = 82$.

and $\frac{\epsilon_U}{\epsilon_S} \geqslant 1$ because of possible full-energy suppression. Values of MDY gain are also plotted (red triangles) in the lower panel of Fig. 4 and one can indeed see that, in some cases, the effect of the gain in detection limit on MDY gain (or identically MDA gain) is reduced to zero (but not negative). Full-energy suppression varies from one peak to the other because the associated transition may or may not belong to an important γ cascade, which leads to varying probabilities of direct Ge-BGO γ-γ coincidences. This is typically the case for the transitions at 415, 985, and 1365 keV which are in coincidence with the $2^+ \rightarrow 0^+$ transition at 1348 keV in ^{82}Ge, or for the 1348 keV transition itself, which is in coincidence with many others. Hence Fig. 4 informs us that, given its geometry and size, this shield, once properly protected from direct exposure to the source, could improve the MDY by ≈21% (as is already the case in some occurrence) on the average. This means that the expected potential improvement is a gain of ≈21% in beam time to achieve identification of the decay of the weakest produced nuclei. Or, put in another way, for a given yield and given beam time, the minimum detectable γ intensity $P_\gamma^{\min}$ is lowered by ≈21% which may help in improving completeness of the deduced level scheme. The usual statements of the little usefulness of Compton rejection in β-delayed γ spectroscopy must be measured in terms of these numbers.

III. RESULTS

A. γ transitions observed in ^{82}Ge decay

The total β-gated γ spectrum obtained in this commissioning run is shown in Fig. 5 and was accumulated over 11 800 iterations of the tape motion (6.56 hours of beam onto the tape only). All the observed activity can be attributed to $A = 82$ isobars decays, with the notable exception of a contaminating ^{132}Sn (and daughters) activity, as explained earlier. We focused our attention on the β decay of ^{82}Ge: γ transitions were attributed to ^{82}As based on half-life measurements of the corresponding γ lines and the γ-γ coincidence measurements, Table II. We confirm the existence of the 249, 843, and 1092 keV transitions initially proposed by Hoff and Fogelberg [1]. They also reported indication only of a 952 keV transition which on the contrary is clearly present in our case. However, similarly to [10], we found no evidence of a 140 keV transition which appears only in [1] as a representation by a dashed line in the level scheme according to which it should be seen in coincidence with the 952 keV transition. The gate around 952 keV on the contrary clearly reveals coincidence with the most intense 1092 keV transition, ruling out the existence of a level at 952 keV. We also confirm all the transitions reported in Ref. [10] except for the one at 421 keV which is attributed to a doublet resolved

TABLE II. γ transitions attributed to the ^{82}Ge decay. Half-live values in the last column were determined from the decay curves of the corresponding lines; the deduced average value $\overline{T}_{1/2}$ (see also Fig. 6) is reported at the bottom of the Table, as well as the evaluated value $T_{1/2}$(lit.).

E_γ (keV)	I_γ (%)	γ-γ	$T_{1/2}$ (s)
92.6(4)	1.0(5)	329.3; 420.4; 426.6; 447.4; 2196.6	3.9 ± 0.6
249.1(5)	3.6(4)	843.4	
329.3(3)	0.5(1)	92.6; 426.6	4.1 ± 1.1
420.4(5)	0.27(9)	92.6; 447.4	3.1 ± 0.8
426.6(2)	0.87(9)	92.6; 329.3; 553.1; 1063.9; 1311.3; 1462.4	4.8 ± 1.1
447.4(3)	0.5(1)	92.6; 420.4	4.9 ± 1.3
516.5(2)	1.25(9)	575.3	4.5 ± 1.6
526.3(3)	0.22(4)	843.4	
553.1(4)	0.20(4)	426.7; 1063.9; 1462.4	
575.3(2)	1.1(1)	516.5	4.0 ± 1.1
843.4(2)	8.0(3)	249.1; 526.3; 1201.1; 1600.1	3.5 ± 0.7
951.8(3)	1.4(4)	1092.0	3.9 ± 1.2
1063.9(3)	0.16(4)	329.3; 426.6; 553.1	
1092.0(2)	100(6)	951.8; 1199.1	5.0 ± 0.7
1199.1(6)	0.5(2)	1092.0	3.4 ± 1.3
1201.1(2)	0.6(2)	843.4	3.9 ± 2.3
1311.3(3)	0.34(7)	329.3; 426.6	4.6 ± 2.3
1462.4(5)	0.31(7)	329.3; 426.6	
1600.1(4)	0.09(2)	843.4	
2196.6(2)	0.12(2)	92.6	
			$\overline{T}_{1/2} = 4.04 \pm 0.27$ s
			$T_{1/2}$(lit.) $= 4.56 \pm 0.26$ s [26]

by coincidence data only. With respect to [10] we identify three new γ lines: at 526.3(3) and 2196.6(2) keV, in addition the line reported in Ref. [10] at 1200.1(3) keV appears in our case as a doublet 1199.1(6)-1201.1(2) keV resolved by the coincidence analysis. The 526.3 keV appears in coincidence with 843.4 keV transition which is the second most intense of the decay scheme with $I_\gamma = 8.0(3)\%$ and allows establishing a new level at 1369.6 keV. The 2196.6 keV line is weak but is visible in a region of the spectrum where the background is low. A coincidence with the 92.6 keV line is clearly established which indicates the existence of anotherlevel at 2420.8 keV not previously reported.

At last we note that the half-life measurement of 13 γ-line decay curves, reported in the last column of Table II and in Fig. 6, amounts to 13 independent measurements of the ^{82}Ge half-life. This allows for a new determination of the ^{82}Ge half-life of $T_{1/2} = 4.04 \pm 0.27$ s with a better accuracy than each of the three previous values available in the literature which have been used so far by the evaluators for the recommended value $T_{1/2}$(lit.) $= 4.56 \pm 0.26$ s [14,26].

B. ^{82}Ge decay scheme

Coincidence relationships of Table II allowed building the ^{82}Ge decay scheme of Fig. 7. The absolute branching ratio I_β to the levels was obtained taking the absolute intensity of the 1092 keV transition $I_\gamma = 80 \pm 20\%$/decay reported in Ref. [27]. They are also reported in Table III along with the corresponding log ft values calculated with the evaluated mass values of [28]. As can be seen, and already noted by Hoff and Fogelberg, the decay of ^{82}Ge is quite selective. Though somewhat augmented, the decay scheme apparently remains still incomplete. As will be discussed in Sec. IV, one could suspect the presence of some other 1^+ states in the Q_β window that could decay by undetected high-energy transitions directly to the ground state, as is the case for the 1092 keV state. For that reason we consider our log ft values as bottom limits only.

The analysis of the activity balances in the $A = 82$ chain from our data suggests that a direct branch towards the ^{82}As ground state is unlikely, which is in agreement with the

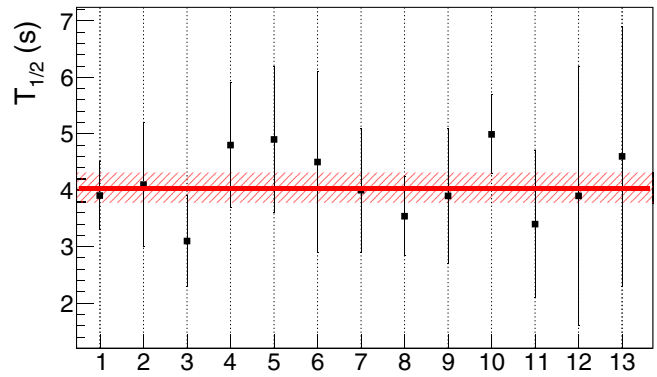

FIG. 6. (Color online) Graphical representation of the last column of Table II. The half-life measurements are numbered on the x axis in the order in which they appear in Table II. The resulting (new) ^{82}Ge half-life determination and associated uncertainty are materialized by the horizontal line and hatched region around $\overline{T}_{1/2} = 4.04 \pm 0.27$ s, to be compared to the evaluated value of 4.56 ± 0.26 s [26].

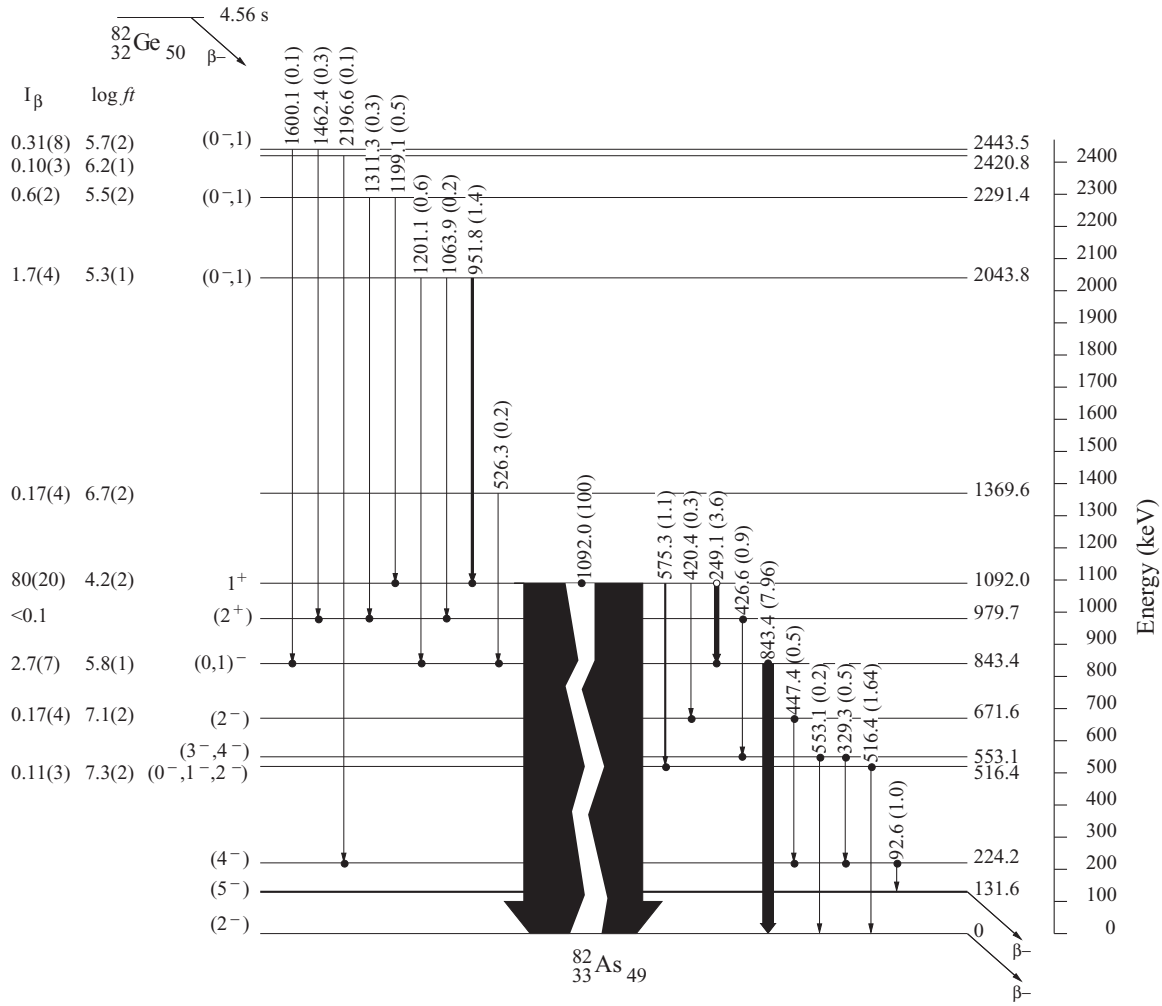

FIG. 7. ^{82}Ge β-decay scheme. Spin-parity assignments to the ground and isomeric (β decaying) states are from Refs. [1,27]. Others are proposed after the discussion in Sec. III B.

original hypothesis of [1] and the recent results of [10]. We will adopt for the rest of the discussion the proposition of $J^\pi = (2^-)$ from [1] for the ground state (and not the 1^+ still present in the evaluation [14]), a proposition further argued in Ref. [27]. The same reference provides convincing arguments for a $J^\pi = (5^-)$ assignment to the isomeric state. In agreement with [10] we suggest that this isomeric state is the same as the one located at 131.6 keV in our level scheme essentially because the recent high-precision mass measurements of ^{82}As and ^{82m}As [29] lead to an energy location of the ^{82}As isomeric state at 128 ± 6 keV and because no γ line is observed at 131.6 keV. At this point some comments are in order on the possible connections between our level scheme and the one obtained from the $(t,^3\mathrm{He})$ reaction studies of Ajzenberg-Selove *et al.* [11]. The floating of the latter in the evaluation is a longstanding problem which, in the final analysis, originally stems from the poor agreement found by Ajzenberg-Selove *et al.* between their (already quite precise) Q value for the formation of the ^{82}As ground state of -7500 ± 25 keV and the (poorly determined) Q_β value available at that time. The integration of recent high-precision mass measurements of ^{82}Se, ^{82}As, and ^{82m}As, especially from [29], in the mass evaluation [28] leads to $Q_\beta(^{82}\mathrm{As}) = 7491(5)$ keV, in remarkable agreement with the

TABLE III. ^{82}As levels populated in the β decay of ^{82}Ge.

Energy (keV)	J^π	I_β (%)	log ft
0	(2^-) [1,27]	0	
131.6(15)	(5^-) [27]	0	
224.2(10)	(4^-)	0	
516.5(2)	$(0^-,1^-,2^-)$	0.11(3)	7.3(2)
553.1(4)	$(3^-,4^-)$	0	
671.6(7)	(2^-)	0.17(4)	7.1(2)
843.4(2)	$(0,1)^-$	2.7(7)	5.8(2)
979.7(6)	(2^+)	0.05(1)	7.5(1)
1092.0(2)	1^+	80(20) [27]	4.2(2)
1369.7(5)		0.17(4)	6.7(2)
2043.8(5)	$(0^-,1)$	1.7(4)	5.25(10)
2291.1(8)	$(0^-,1)$	0.6(2)	5.5(2)
2420.8(12)		0.10(3)	6.2(1)
2443.5(6)	$(0^-,1)$	0.31(8)	5.7(2)

Q value obtained by Ajzenberg-Selove *et al.*. We note that the latter was not used for the 2012 mass evaluation and there is no possible biasing. According to this, the group labeled 0 in the spectrum of Fig. 3 in Ref. [11] is almost certainly due to the ^{82}As ground state. Apparently the isomeric state was in fact also well populated in the $(t,^3\mathrm{He})$ reaction and would correspond to the group labeled 1, at 124 ± 15 keV excitation energy, in the ^{3}He spectrum of [11]. Further discussion on the complementarity of the two level schemes from radioactivity and transfer reactions will be found in Sec. IV.

The 1092 keV level clearly attracts most of the β strength and cannot be anything else than a 1^+ state as initially proposed in Ref. [1]. If the (2^-) assignment to the ground state is correct, the direct transition from this 1^+ state to the ground state must have an $E1$ nature. Below 1 MeV only the level at 843 keV is distinguished by a sizable direct β population. However, the branching ratio is much lower than in the case of the 1092 keV level, and the lower limit of $\log ft > 5.8$ we obtain clearly excludes the usual range for allowed transitions. Should the 843 keV level correspond to a first excited 1^+ state as proposed by Hoff and Fogelberg, it would attract much more β population as the Q_β window is even larger than for the 1092 keV level. In addition, the relative intensities of the 249 and 1092 keV transitions depopulating the 1^+ state at 1092 keV have a ratio $I(249)/I(1092) \approx 4\%$. It is compatible with the ratio of the Weisskopf estimates of two $E1$ 249 and 1092 keV transitions. Assuming that the 1092 keV transition is $E1$ as explained above, the probability of a $M1$ transition of 249 keV would have been four orders magnitude lower and would have not been detected. This argument is also in favor of a negative parity for the 843 keV level. We propose then to assign to it $J^\pi = (0,1)^-$; a positive parity seems to us totally excluded.

Apart from the 1092 keV level, the only $\log ft$ values which could indicate allowed β transitions concern the three levels at 2044, 2291, and 2443 keV. As they lie higher in the level scheme they might be less subject to Pandemonium population. Then we consider them as reasonable candidates for a $J^\pi = 1^+$ assignment, though 0^- or 1^- cannot be excluded definitively (a $0^+ \rightarrow 0^+$ transition is obviously excluded as the very high degree of forbiddenness to which it corresponds lies far beyond our detection limits and statistics).

The 224 keV level apparently receives no direct population. It decays to the isomeric state with proposed $J^\pi = (5^-)$ [27] by a low energy, 93 keV transition and not to the (2^-) ground state. Only $E1$ or $M1$ transitions at such energy would prevent this 224 keV state from becoming isomeric. There are no proton and neutron orbits close to the Fermi level which could generate 4^+ to 6^+ states at this energy hence an $E1$ transition seems excluded and the 93 keV transition is most likely of $M1$ nature. In agreement with [10] we propose $J^\pi = (4^-)$ for the 224 keV level.

Tentative spin-parity assignments to the rest of the level scheme are more difficult. The 516 keV level receives population from the well established 1^+ state at 1092 keV and decays solely to the (2^-) ground state. It receives very weak apparent direct β population, if it receives any. In the hypothesis that this direct population is real one must assume that it comes through a first-forbidden nonunique, or even unique, β transition. We propose then $J^\pi = (0^-,1^-,2^-)$ for this level.

According to our intensity balance, the level at 553 keV has no direct feeding at all; actually our balance is negative and this state must decay by a supplementary transition we did not observe. Miernik *et al.* report the existence of a component in the peak at 420 keV which could correspond to an additional transition deexciting this state towards the (5^-) state at 132 keV of which we find no evidence in our spectra. We then adopt for the following their spin-parity proposition for this level, $(3^-,4^-)$.

The 672 keV level corresponds to a very tiny β branch and the actual $\log ft$ could be considerably higher than the lower limit of 7.1 we determined. It receives population from the well established 1^+ state at 1092 keV and decays towards the previously proposed $J^\pi = (4^-)$ level at 224 keV. A $J^\pi = (2^-)$ assignment seems then reasonable.

At last we comment the state located at 980 keV excitation energy: interestingly it is the only state of the level scheme which attracts population from the three high-lying (1^+) states simultaneously. The direct β population is practically negligible and a first-forbidden non-nique transition seems unlikely, otherwise one would have observed a β branch of intensity similar to the one feeding the close lying 843 keV level. In addition it is the only level in the group from 516 to 1092 keV which is connected to none of the lower lying triplet of states. This suggests a different structure for this state, maybe a different parity. We hence very tentatively propose $J^\pi = (2^+)$ for the 980 keV level.

IV. DISCUSSION

As explained in the Introduction, our study was originally focused on the sudden occurrence in the light $N = 49$ odd-odd isotonic chain of a large number of low lying 1^+ states in ^{80}Ga by providing a reliable intermediate example, viz., ^{82}As. The improved knowledge of the higher energy part of the ^{82}As level scheme from the present work allows suspecting the existence of (only) three additional, potential 1^+ states above the already known one at 1092 keV. In addition our data allow ruling out the hypothesis that the 843 keV level could be a 1^+ state. The question now is to understand this new level scheme and also try and understand the differences between it and the one from transfer reaction data.

A. Regional considerations and zero-order couplings

A first step towards a real understanding of the ^{82}As structure would be to look at the approximate location of the unperturbed proton-neutron multiplet centroids. For that purpose one needs to identify in the experimental level schemes of the odd-proton $N = 50$ and odd-neutron $N = 49$ nuclei the levels which can correspond to the proton quasiparticle (QP) states and the 1h and 1p-2h neutron states respectively. For neutron states we simply adopt the systematics proposed in Refs. [1–3]. In ^{81}Ge one looses track of the exact position of the $2p_{3/2}$ and $1f_{5/2}$ 1h states as there is an ambiguity on the possible nature of the $3/2^-$ and $5/2^-$ states at 1724 and 1832 keV since they could also originate from the core-coupled

TABLE IV. Proton QP energies E_{QP} and occupation probabilities v^2 for the $N = 50$ odd isotones. Values were obtained with BCS equations resolved to reproduce the experimental paring gap as indicated in the second line. E_{exp} are the energies of the corresponding states in the experimental level schemes. All energies are in MeV.

Nucleus (Δ_p)	^{87}Rb (0.996)		^{85}Br (1.031)		^{83}As (1.012)		^{81}Ga (0.904)	
QP	E_{QP} v^2	E_{exp}	E_{QP} v^2	E_{exp}	E_{QP} v^2	E_{exp}	E_{QP} v^2	E_{exp}
$2p_{3/2}$	0.0	0.0	0.0	0.0	0.280	0.306	(0.810)	0.351
	0.81		0.40		0.19		(0.08)	
$1f_{5/2}$	0.376	0.402	0.361	0.345	0.0	0.0	0.0	0.0
	0.90		0.84		0.66		(0.43)	
$2p_{1/2}$	0.802	0.845	1.357	1.191	1.474	1.257	(2.119)	
	0.06		0.05		0.03		(0.02)	
$1g_{9/2}$	1.658	1.578	1.958	1.859	2.883	2.776	(3.542)	
	0.03		0.03		0.02		(0.01)	

$2^+_1 \otimes 2p_{1/2}$ configuration. We hence use these values as lower limits only. For proton states one can use the single particle energies obtained from transfer reaction in Ref. [30] and calculate the corresponding QP state using BCS equations and the pairing gap extracted from experimental mass data to help in the identification in the most likely candidates in the level schemes. The results are summarized in Table IV. For ^{81}Ga, information is too scarce for a proper identification. ^{81}Ga is also too far from the reference measurements of Ref. [30] to securely extrapolate the single-particle energies, hence the BCS values are given in Table IV in parentheses as an indication only. We will use only the first known excited state as candidate for the $2p_{3/2}$ QP state as already suggested in Ref. [31]. The zeroth-order coupling energies of the relevant proton-neutron configurations are represented in Fig. 8 for $31 \leqslant Z \leqslant 37$. The experimental energy of the first firmly identified 1^+_1 state in those odd-odd nuclei is also reported for comparison. One sees a remarkable agreement between the energy evolution of this 1^+_1 state and that of the proton QP $2p_{3/2}$ – neutron 1h $2p_{1/2}$ (considered thereafter as a 2QP state noted $\tilde{\pi}2p_{3/2} \otimes \tilde{\nu}2p_{1/2}$) zeroth-order coupling centroid. The second very interesting feature is that ^{82}As is the first of the $N = 49$ odd-odd nuclei series (going down in Z) for which zeroth-order centroids of negative parity configurations involving neutron orbitals stemming from above the $N = 50$ shell closure $\tilde{\pi} \otimes \tilde{\nu}\{2d_{5/2}, 3s_{1/2}, 2d_{3/2}\}$ (thereafter called "intruder" configuration, in that sense that they do not belong to the natural valence space) come lower in energy than the natural positive parity configurations. This comes essentially from the fact that while the energies of all the neutron 1h states systematically increase for $Z \leqslant 34$, all neutron 1p-2h states have minimal energies at mid proton (28-40) shell, $Z \approx 34$. These intruder configurations will generate $J^\pi \leqslant 1^-$ states which are very likely to be populated by first-forbidden β transitions. These (still) crude arguments provide a first hint for the possible origin of an increase of the occurrence of a large number of low-lying low-spin states populated in β decay starting from ^{82}As and increasing in ^{80}Ga. As will be seen in the next subsection the ubiquitous presence of these intruder states impedes any effort to describe ^{82}As (and even

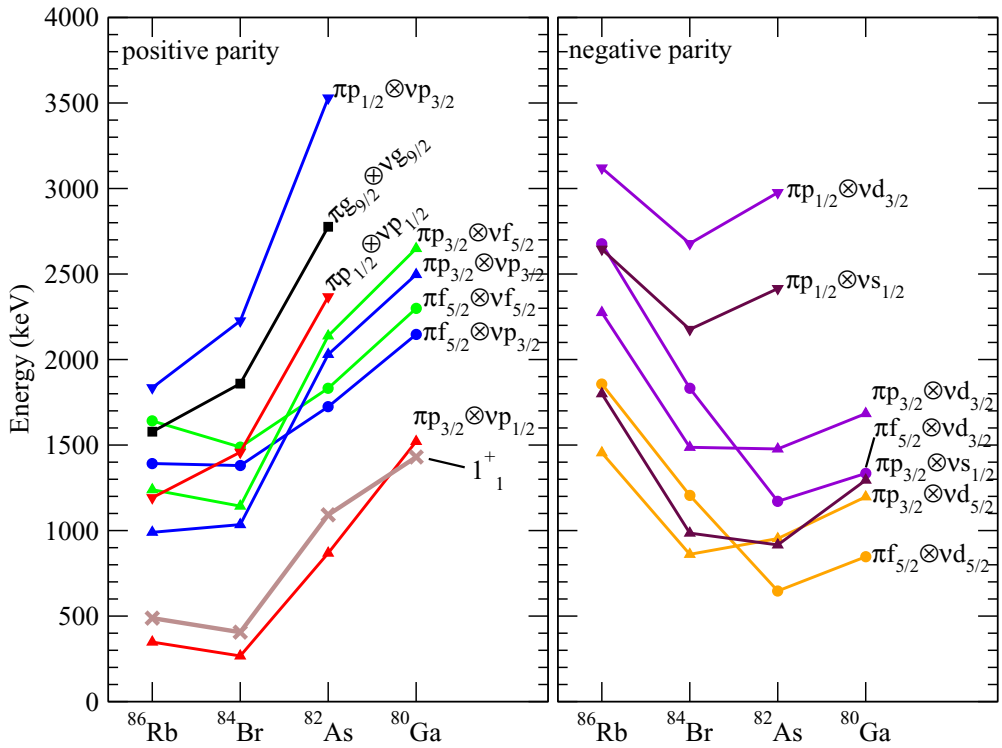

FIG. 8. (Color online) Unperturbed energy positions of the QP proton and neutron 1h (left panel) and 1p-2h (right panel) zeroth-order coupling centroids in the $N = 49$ odd-odd nuclei with $31 \leqslant Z \leqslant 37$.

more ^{80}Ga) with shell model calculations restricted to the ^{56}Ni natural valence space, whatever the sophistication of the interaction used.

B. ^{82}As within the shell model

In first approximation the low energy structure of ^{82}As should belong to the natural valence space of ^{56}Ni spanned by the proton and neutron $1f_{5/2}$,$2p_{3/2}$,$2p_{1/2}$ and $1g_{9/2}$ orbitals. The structure of the light odd-odd $N = 49$ isotones, from ^{88}Y to ^{80}Ga, has been discussed in detail by Honma *et al.* [32] in the framework of shell model calculations performed precisely in this valence space. However, even on the question restricted to the number and energy reproduction of the low-lying 1^+ states one is quickly disappointed. As pointed out by Honma *et al.*, already for the experimentally extensively studied ^{88}Y the correct description of the 1^+_1 state is a long identified problem in the shell model (see [32] and references therein) that, surprisingly enough, the net improvement for the global description of this mass region that constitutes the introduction of the JUN45 interaction does not help solve completely. An interesting way out, suggested by these authors, would be the inclusion of intruder 1p-2h (across the $N = 50$ gap) states in the calculations. Such large-scale shell model calculations are becoming available but are still limited to the inclusion of the $\nu 2d_{5/2}$ orbital (see, e.g., [33]). The systematic presence and energy evolution of positive parity $(1/2^+,3/2^+,5/2^+)$ 1p-2h states pointed out in [1] and [2] already a long time ago and the results of the previous subsection strongly suggest the necessity to include also the $\nu 3s_{1/2}$ and $2d_{3/2}$ orbitals for a proper description of the $N = 49$ isotones. Miernik *et al.* [10] present a systematic comparison of the ^{82}As experimental level scheme with several shell model calculations, using very different interactions, but all performed in the fpg valence space: the systematically (very) poor agreement with the ^{82}As experimental level scheme obtained also points towards the absence of essential parts of the ^{82}As structure in the ^{56}Ni natural valence space.

For that reason and (i) in order to keep a physical image close at hand (a necessity when dealing with the complex spectroscopy of odd-odd nuclei) and (ii) to be able to pin down the proton-neutron configurations of major influence, we have decided to apply the core-coupling model to the description of the $N = 49$ odd-odd nuclei. In this approach, the inclusion of several intruder configurations can be done conveniently at low computational cost. This last-resort solution allows waiting for possible ambitious large scale shell model calculations.

C. Core-coupling approach

Our work was encouraged and somewhat facilitated by the three following facts:

(i) the study of the coupling of 1h and 1p-2h neutron states to $N = 50$ even-even cores for the description of $N = 49$ odd nuclei is already available down to ^{85}Kr [34,35];

(ii) Hoffmann-Pinther and Adams [36] have already treated successfully the case of an odd-odd nucleus in this region, viz., ^{90}Y, within a core-coupling approach using the Thankappan-True schematic core-particle interaction [37];

(iii) The proton-neutron multiplets have been identified in the $N = 49$ nucleus ^{86}Rb with reasonable certainty [38,39], providing a reference point for the calculations.

The Hamiltonian used for the description of the odd-odd $N = 49$ nuclei is the one described in Ref. [36] (which we reproduce here for the sake of convenience):

$$\begin{aligned} H &= H_c + H_p + H_n + H_{pc} + H_{nc} + H_{np}, \\ H &= H_c + H_p + H_n \\ &\quad -\xi_p \mathbf{J}_c \cdot \mathbf{j}_p - \eta_p \mathbf{Q}_c \cdot \mathbf{Q}_p - \xi_n \mathbf{J}_c \cdot \mathbf{j}_n - \eta_n \mathbf{Q}_c \cdot \mathbf{Q}_n \\ &\quad + V_0[(1-\alpha) + \alpha(\boldsymbol{\sigma}_p \cdot \boldsymbol{\sigma}_n)]\delta(\mathbf{r}_p - \mathbf{r}_n), \end{aligned} \tag{1}$$

with the extension to quasiparticle representation introduced in Ref. [40]. In Eq. (1), H_c, H_p, and H_n are the Hamiltonians of the core, the odd proton QP, and the odd neutron QP respectively. $\mathbf{J}_c$ and $\mathbf{j}_n$ ($\mathbf{j}_p$) correspond to the angular momenta of the core and the neutron QP (the proton QP). $\mathbf{Q}_{n,p}$ are the quadrupole operators for the proton QP and the neutron QP.

^{82}As was taken to be a ^{82}Ge core plus one neutron and one proton QP. Proton $\{1f_{5/2},2p_{3/2},2p_{1/2},1g_{9/2}\}$ and neutron $\{2p_{1/2},1g_{9/2},2d_{5/2},3s_{1/2},2d_{3/2}\}$ QP states were taken into account in the calculation. The core states were restricted to the ground 0^+ and first excited 2^+ states only in order to keep a reasonable number of core coupling parameters. In such a condition and following the approach of Thankappan and True [37] it is convenient to further parametrize the reduced matrix elements of the quadrupole operator $\mathbf{Q}_c$ in the following form:

$$\begin{aligned} \chi_1 &= \eta \langle 0^+ \| \mathbf{Q}_c \| 2^+ \rangle, \\ \chi_2 &= \eta \langle 2^+ \| \mathbf{Q}_c \| 2^+ \rangle. \end{aligned}$$

Hence the coupling strength is described by six parameters: ξ_p, χ_{1p}, χ_{2p} for protons and ξ_n, χ_{1n}, χ_{2n} for neutrons. These parameters were first adjusted to reproduce the experimental level schemes of ^{83}As and ^{81}Ge respectively. The proton-neutron delta interaction parameters were taken from [38] as they were shown to reproduce the 2^--7^- energy splitting of the $\pi 1f_{5/2} \otimes \nu 1g^{-1}_{9/2}$ configuration. Before going to the ^{82}As case we have checked that the ^{86}Rb level scheme could be reproduced by this core+2QP approach considering this nucleus as a ^{86}Kr core plus one neutron and one proton QP. The coupling strength parameters were adjusted to reproduce mainly the splitting of the first $2^+ \otimes j_{\text{lowest}}$ multiplet in the two odd nuclei, namely, in the case of ^{86}Rb: ^{85}Kr and ^{87}Rb. The results of these adjustments are displayed in Fig. 9, and the corresponding parameters summarized in Table V. The final result for ^{86}Rb is shown graphically in Fig. 10.

One of the main underlying hypotheses of the model is that the core state contains sufficiently fragmented components of the particle states to which it is coupled so that blocking or polarization effects remain limited. This condition is approximately fulfilled when core states wave functions correspond to a closed shell configuration mainly. In the case of interest for us here, the core neutron shell is closed while the core

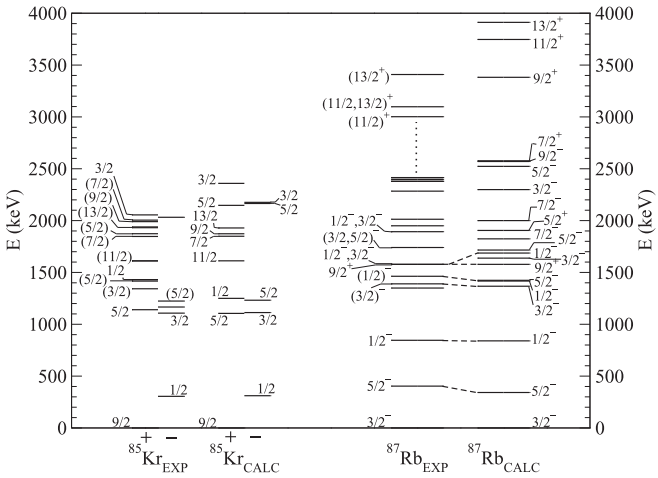

FIG. 9. Comparison between experimental and calculated level schemes for the odd neutron (^{85}Kr, left-hand part) and odd proton (^{87}Rb, right-hand part) neighbors of ^{86}Rb. Positive and negative parity levels are separated in two distinct columns (noted "+" and "−") in the case of ^{85}Kr for the sake of clarity. The theoretical level schemes are obtained after adjustment of the core-QP strength parameters and QP energies. The fitted parameters are then used directly for the core+2QP calculation.

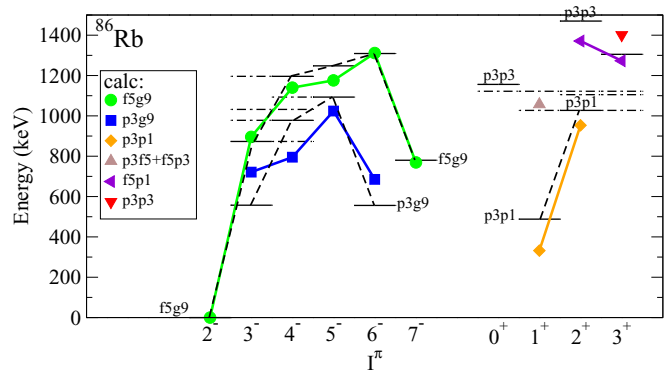

FIG. 10. (Color online) Experimental and calculated level schemes for ^{86}Rb sorted as a function of spin and parity. Experimental data are taken from [39]. In case of experimental uncertainty in the spin determination dashed dotted lines spanning over the corresponding spin range are used to represent the level. Labels close to the experimental levels correspond to their experimentally assigned [38,39] proton-neutron multiplet belonging. A label such as f5g9 stands for $\tilde{\pi}1f_{5/2} \otimes \tilde{\nu}1g_{9/2}$ and so on. Experimental levels belonging to the same proton-neutron configuration are connected by dashed lines. The symbols superimposed are the energies obtained from the core-coupling calculations. States having their leading component along a given core-coupled vector $|(j_{\tilde{\pi}}\, j_{\tilde{\nu}})I \otimes 0^{+}_{\text{core}}; I\rangle$ are connected by a continuous line. Corresponding labels (with the same meaning as for the experimental levels) are given in the legend box "calc".

proton shell is fully opened. In Ref. [36] blocking effects were absorbed by core and single-particle energies modifications in the case of the odd-odd nucleus with respect to the values determined for the two neighboring odd nuclei. From our study of ^{86}Rb as ^{86}Kr + 2QP it is seen that these effects can be absorbed somehow by letting the occupation coefficient v^2 of the proton orbital closest to the Fermi level vary slightly from the reference value in the odd case. This is the only parameter that was slightly adjusted when moving to the odd-odd case once all other parameters have been adjusted for the two odd neighbor nuclei. The results of the adjustments to the two odd

TABLE V. Summary of the core+2QP parameters used for the calculations of ^{86}Rb and ^{82}As nuclei.

Nucleus	Quasiparticles			coupling parameters					
(Core)	l_j	E_{lj} (MeV)	v^2	ξ_p (MeV)	χ_{1p} (MeV fm^{-2})	χ_{2p} (MeV fm^{-2})	ξ_n (MeV)	χ_{1n} (MeV fm^{-2})	χ_{2n} (MeV fm^{-2})
^{86}Rb	$\tilde{\pi}\, p_{3/2}$	0.0	0.72	−0.092	0.151	−0.158	−0.016	0.211	−0.135
(^{86}Kr)	$\tilde{\pi}\, f_{5/2}$	0.376	0.90						
	$\tilde{\pi}\, p_{1/2}$	0.802	0.06						
	$\tilde{\pi}\, g_{9/2}$	1.658	0.03						
	$\tilde{\nu} g_{9/2}$	0.0	0.91						
	$\tilde{\nu} p_{1/2}$	0.410	0.95						
	$\tilde{\nu} p_{3/2}$	1.220	0.98						
	$\tilde{\nu} f_{5/2}$	1.310	0.98						
	$\tilde{\nu} d_{5/2}$	1.308	0.02						
	$\tilde{\nu} s_{1/2}$	2.013	0.01						
	$\tilde{\nu} d_{3/2}$	2.978	0.01						
^{82}As	$\tilde{\pi}\, p_{3/2}$	0.280	0.40	−0.053	0.116	0.105	0.015	0.090	−0.127
(^{82}Ge)	$\tilde{\pi}\, f_{5/2}$	0.0	0.50						
	$\tilde{\pi}\, p_{1/2}$	1.474	0.04						
	$\tilde{\pi}\, g_{9/2}$	2.883	0.02						
	$\tilde{\nu} g_{9/2}$	0.0	0.95						
	$\tilde{\nu} p_{1/2}$	0.610	0.98						
	$\tilde{\nu} d_{5/2}$	0.743	0.20						
	$\tilde{\nu} s_{1/2}$	0.789	0.10						
	$\tilde{\nu} d_{3/2}$	1.333	0.05						

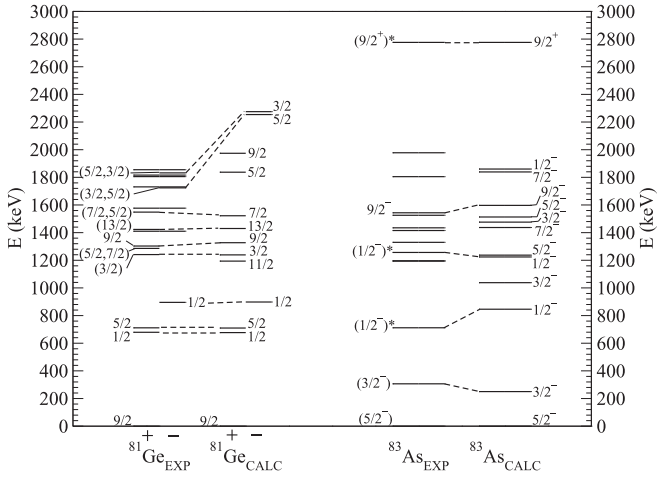

FIG. 11. Same as Fig. 9 for the case of ^{82}As [tentative spin-parity assignments marked by asterisks (∗) are from us].

proton and odd neutron neighbors of ^{82}As are displayed in Fig. 11 and the corresponding parameters are summarized in Table V. The final result for ^{82}As is shown graphically in Fig. 12.

The most important information from this figure is that below 1 MeV, apart from the 2^- ground state, low-spin negative parity states with $J^\pi \leqslant 2^-$ cannot be due to normal configurations and must necessarily stem from intruder ones, involving $2d_{5/2}$,$3s_{1/2}$ neutron QPs. This was expected qualitatively from the zero-order coupling energy analysis of Sec. IV A. The only other possibilities to generate $J^\pi \leqslant 2^-$ states are from $[(\tilde{\pi}\,1f_{5/2} \otimes \tilde{\nu}\,1g_{9/2})_{\{2,3,4\}} \otimes 2^+_{\rm core}]$ configurations, but none of them is sufficiently favored in energy. The core + 2QP model predicts a large density of 2^- states but they lie higher in energy than the experimental candidates. However, it clearly predicts the presence of a 0^- and a 1^- state around ≈850 keV.

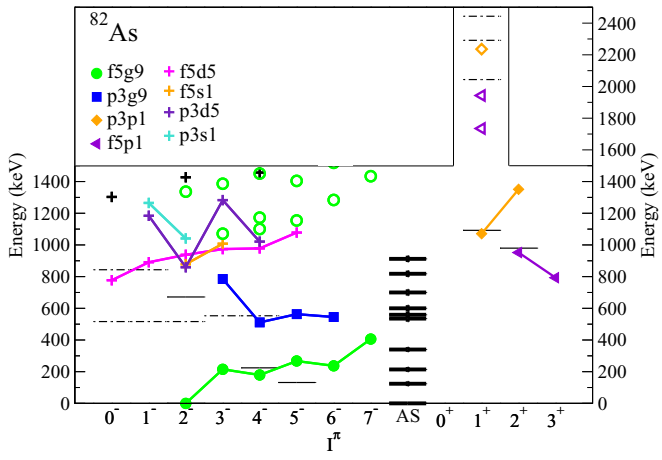

FIG. 12. (Color online) Calculated and experimental levels of ^{82}As; see legend of Fig. 10 for explanations. The experimental levels with no definite J^π assignment, noted "AS" are from [11]. The open symbols correspond to states having their leading component along a given core-coupled vector $|(j_{\tilde{\pi}}\,j_{\tilde{\nu}})j_{\pi\nu} \otimes 2^+_{\rm core}; I\rangle$. The shapes of the open symbols are those of the corresponding $(j_{\tilde{\pi}}\,j_{\tilde{\nu}})$ configurations.

The experimental level at 843 keV for which we proposed $J^\pi = (0,1)^-$ (firm negative parity) most certainly belongs to the intruder $(\tilde{\pi}\,1f_{5/2} \otimes \tilde{\nu}2d_{5/2})$ multiplet. The 516 and 672 keV levels, proposed as $J^\pi = (0^-,1^-,2^-)$ and (2^-) respectively must also belong to an intruder configuration though the poor agreement obtained with the calculations prevents from proposing a definitive configuration. It is interesting to note, consistently with Fig. 8, that close to the middle of the $f_{5/2},p$ proton subshell, just next to the $N = 50$ shell closure, the first intruder configuration appears at as low an energy as ≈0.5 MeV.

The rest of the negative parity state structure deserves some comment. The ground 2^- state undoubtedly belongs to the $(\tilde{\pi}\,1f_{5/2} \otimes \tilde{\nu}\,1g_{9/2})$ normal configuration multiplet. It is the same configuration as the one of the 2^- ground state of ^{86}Rb. This simply reflects the fact that the orientation of the corresponding Paar parabola is not yet inverted at $Z = 33$. Inversion has certainly occurred at $Z = 31$ as the $J^\pi = 6^-$ member of the multiplet has become the ground state in ^{80}Ga [8] consistently with the fact that the $\pi\,1f_{5/2}$ occupation coefficient must have become <0.5. Furthermore the (4^-) state at 224 keV and isomeric (5^-) state at 132 keV cannot belong to anything else than the ground $(\tilde{\pi}\,1f_{5/2} \otimes \tilde{\nu}\,1g_{9/2})$ configuration. The calculated order of the 4^- and 5^- states is reversed with respect to the experimental one: any detail in the actual proton-neutron interaction could lead to this effect and it is clear that the simple contact interaction used here cannot reproduce all of them. The experimental level at 553 keV excitation energy, attributed to $J^\pi = (3^-,4^-)$, lies very close to the calculated $J^\pi = 4^-$ member of the $(\tilde{\pi}\,2p_{3/2} \otimes \tilde{\nu}\,1g_{9/2})$ normal configuration. At last, we note also that the ^{82}Se$(t,^3$He$)^{82}$As reaction should favor the population of the two normal configurations $(\tilde{\pi}\,1f_{5/2} \otimes \tilde{\nu}\,1g_{9/2})$ and $(\tilde{\pi}\,2p_{3/2} \otimes \tilde{\nu}\,1g_{9/2})$ multiplets. The calculated level density and energy range of these states match very nicely the experimental level scheme of [11]: while Ajzenberg-Selove *et al.* report the observation of 10 (or 11) levels, those two configurations generate naturally the 10 first negative parity states of the theoretical level scheme (see Fig. 12). However, the agreement remains at a qualitative level only, since no spin-parity assignments to those levels have been proposed in Ref. [11] and one cannot expect a perfect reproduction of all the fine details of the multiplet splittings with such a simple proton-neutron interaction [see, e.g., the distortion of the $(\tilde{\pi}\,2p_{3/2} \otimes \tilde{\nu}\,1g_{9/2})$ multiplet in ^{86}Rb, Fig. 10].

Concerning now the positive parity state structure, the 1^+ state identified at 1092 keV lies very close to the calculated 1^+ state stemming from the $(\tilde{\pi}\,2p_{3/2} \otimes \tilde{\nu}\,2p_{1/2})$ configuration. This state would then have the same nature as the first 1^+ state in ^{86}Rb; this is consistent with the 1^+_1 experimental systematics and zeroth-order energy evolutions of Fig. 8. The experimental level at 980 keV very tentatively assigned to $J^\pi = (2^+)$ lies very close in energy to the calculated 2^+ member of the $(\tilde{\pi}\,1f_{5/2} \otimes \tilde{\nu}\,2p_{1/2})$ normal configuration and could be indeed naturally attributed to this configuration. In Fig. 12 we also show higher lying calculated 1^+ states. These states originate from the couplings of the lowest positive parity $(\tilde{\pi}\,1f_{5/2} \otimes \tilde{\nu}\,2p_{1/2})$ and $(\tilde{\pi}\,2p_{3/2} \otimes \tilde{\nu}\,2p_{1/2})$ configurations to the 2^+_1 core excitation. The three experimental 1^+ candidates

at 2044, 2291, and 2443 keV could then be attributed to these excited core couplings. However we remind here, as already noted earlier, that in ^{81}Ge one misses experimental evidence of the exact position of the $2p_{3/2}$ and $1f_{5/2}$ 1h states. Hence it is possible also that these three experimental states actually reveal the approximate energy locations of these 1h states. Consequently no firm conclusion can be drawn for those three experimental 1^+ state candidates.

For that reason and for a more reliable discussion on the origin of the 1^+ states in ^{82}As we have chosen to study the influence of higher lying quasiparticle states and 2h-2p configurations within a fully microscopic approach as described in the following subsection. Calculations are also extended to the case of ^{80}Ga to shed light on the significant increase, from ^{82}As to ^{80}Ga, of the number of states directly populated in β decay, as noted in the Introduction.

D. QRPA description

It is helpful to study the effects of the configuration space on the low-energy spectrum of 1^+ excitations in ^{80}Ga and ^{82}As. In this section our tool is the quasiparticle random phase approximation (QRPA) with Skyrme interactions treated in a finite-rank separable approximation (FRSA) [41,42]. Making use of the FRSA [43] for the residual interaction enables one to perform QRPA calculations in very large two-quasiparticle (2QP) spaces. In particular, the cutoff in the discretized single-particle (s.p.) continuum can be chosen at 100 MeV. Using the general scheme of the quasiparticle-phonon model (QPM) [44,45] with Skyrme-type interactions as inputs, the Hamiltonian can be diagonalized in a space spanned by states composed of one and two QRPA phonons [46],

$$\Psi_\nu(\lambda\mu) = \left(\sum_i R_i(\lambda\nu) Q^+_{\lambda\mu i} + \sum_{\lambda_1 i_1 \lambda_2 i_2} P^{\lambda_1 i_1}_{\lambda_2 i_2}(\lambda\nu) \left[Q^+_{\lambda_1\mu_1 i_1} \bar{Q}^+_{\lambda_2\mu_2 i_2} \right]_{\lambda\mu} \right) |0\rangle, \quad (2)$$

where λ denotes the total angular momentum and μ is its z projection in the laboratory system. The ground state of the parent (even-even) nucleus is the QRPA phonon vacuum $|0\rangle$. The wave functions $Q^+_{\lambda\mu i}|0\rangle$ of the one-phonon excited states of the daughter (odd-odd) nucleus are described as linear combinations of 2QP configurations; $\bar{Q}^+_{\lambda\mu i}|0\rangle$ is a one-phonon electric excitation of the parent nucleus. To construct the two-phonon excitations we build the $[1^+_i \otimes \lambda^+_{i'}]_{\rm QRPA}$ operators with $\lambda = 0,2$. The amplitudes $R_i(\lambda\nu)$ and $P^{\lambda_1 i_1}_{\lambda_2 i_2}(\lambda\nu)$ are determined from the variational principle, which leads to a set of linear equations [46]. The equations have the same form as the QPM equations, but the s.p. spectrum and the parameters of the residual interaction are obtained from the chosen Skyrme forces without any further adjustments.

Using the same ansatz as Sec. II of Ref. [47], the excitation energies of the 1^+_ν states with respect to the daughter ground state are given by

$$E_{1^+_\nu} \approx E_\nu - E_{\rm 2QP,lowest}, \quad (3)$$

TABLE VI. Energies and dominant components of phonon structures of the $1^+_{1,2}$ states in ^{80}Ga and ^{82}As. The states are calculated with inclusion the phonon-phonon coupling (2). Experimental data of ^{80}Ga are taken from Ref. [8].

	$\lambda^\pi_i = 1^+_i$	Energy (MeV)		Structure
		Expt.	Theory	
^{80}Ga	1^+_1	0.708	1.0	$81\%[1^+_1]_{\rm QRPA}$
	1^+_2	1.450	2.9	$38\%[1^+_3]_{\rm QRPA}$ $+35\%[1^+_1 \otimes 2^+_1]_{\rm QRPA}$
^{82}As	1^+_1	1.092	0.6	$76\%[1^+_1]_{\rm QRPA}$
	1^+_2	2.044	2.1	$30\%[1^+_1 \otimes 2^+_1]_{\rm QRPA}$ $+24\%[1^+_3]_{\rm QRPA}$

where E_ν are the eigenvalues of the QRPA equations, or of the equations taking into account the two-phonon configurations (2), and $E_{\rm 2QP,lowest}$ denotes the lowest 2QP energy. It is worth mentioning that the spin-parity of the lowest 2QP state is, in general, different from 1^+. In the same approximation [47], the Q_{β^-} value is calculated by the following expression:

$$Q_{\beta^-} \approx \Delta M_{n-H} + \mu_n - \mu_p - E_{\rm 2QP,lowest}, \quad (4)$$

where $\Delta M_{n-H} = 0.782$ MeV is the mass difference between the neutron and the hydrogen atom, μ_n and μ_p are the neutron and proton chemical potentials, respectively.

In Ref. [46], this approach was applied to study the combined influence of the coupling between one- and two-phonon terms in the wave functions (2), and of the tensor force effects on the Gamow-Teller (GT) strength distributions in the Q_β window of ^{80}Zn and ^{82}Ge. Here, we briefly summarize the details of the calculations. The pairing correlations are generated by a zero-range volume force, fixed in Refs. [46,48]. In the particle-hole channel we use the central Skyrme interaction SGII [49] and the same zero-range tensor interaction as in Ref. [50]. The SGII parametrization is known to give a rather satisfactory description of spin-related properties. In particular, one obtains a good description of experimental energies of the GT resonances in ^{90}Zr. The tensor force has been added perturbatively to the standard parametrization SGII in order to improve the description of the energy differences of the $1h_{11/2}$ and $1g_{7/2}$ proton states in Sn isotopes and the $1i_{13/2}$ and $1h_{9/2}$ neutron states in $N = 82$ isotones [50,51]. A strong tensor interaction results in a rather satisfactory agreement with the β-decay half-lives of ^{80}Zn (0.1 s) and ^{82}Ge (2.4 s) [46]. Since the largest contribution in the calculated half-lives comes from the 1^+_1 state, it is very important to describe the energy and phonon composition of the 1^+_1 state correctly (see Table VI). The crucial contribution in the wave function of the first 1^+ states of ^{80}Ga and ^{82}As comes from the $[1^+_1]_{\rm QRPA}$ configuration, while the two-phonon contributions are also appreciable. The second 1^+ states are dominated by the two-phonon configuration $[1^+_1 \otimes 2^+_1]_{\rm QRPA}$. Thus, the extension of the variational space from the standard QRPA to include the two-phonon configurations has a strong effect on the $1^+_{1,2}$ structure of ^{80}Ga and ^{82}As.

TABLE VII. Energies and structures of the QRPA dipole states in ^{80}Ga and ^{82}As. 2QP configuration contributions greater than 15% are given.

	State	Energy (MeV)	Structure
^{80}Ga	$[1^+_1]_{\rm QRPA}$	1.8	$53\%\{\pi 2p_{3/2}\nu 2p_{1/2}\}$
	$[1^+_2]_{\rm QRPA}$	3.7	$32\%\{\pi 2p_{3/2}\nu 2p_{1/2}\}$
			$30\%\{\pi 1f_{5/2}\nu 1f_{5/2}\}$
			$15\%\{\pi 2p_{3/2}\nu 1f_{5/2}\}$
	$[1^+_3]_{\rm QRPA}$	3.9	$32\%\{\pi 2p_{3/2}\nu 1f_{5/2}\}$
			$30\%\{\pi 1f_{5/2}\nu 1f_{5/2}\}$
			$25\%\{\pi 1f_{5/2}\nu 2p_{3/2}\}$
	$[1^+_4]_{\rm QRPA}$	3.9	$28\%\{\pi 1f_{5/2}\nu 2p_{3/2}\}$
			$27\%\{\pi 1f_{5/2}\nu 1f_{5/2}\}$
			$16\%\{\pi 2p_{3/2}\nu 2p_{3/2}\}$
			$15\%\{\pi 2p_{3/2}\nu 1f_{5/2}\}$
^{82}As	$[1^+_1]_{\rm QRPA}$	1.7	$64\%\{\pi 2p_{3/2}\nu 2p_{1/2}\}$

The energies and wave-function structure of all the QRPA 1^+ states appearing in the calculated Q_β window are given in Table VII. The QRPA results indicate a collective character for the $[1^+_1]_{\rm QRPA}$ state with the dominance of the $\{\pi 2p_{3/2}\nu 2p_{1/2}\}$ configuration which is split between the $[1^+_{1,2}]_{\rm QRPA}$ states. Note that the lowest 2QP state $\{\pi 1f_{5/2}\nu 1g_{9/2}\}$ has a spin and a parity different from 1^+. An overestimation of the experimental $1^+_{1,2}$ energies within the QRPA calculations (see Table VI) indicates that there is room for two-phonon effects. In other words, the one-phonon analysis shown in Table VII is a rough estimate only. The $[1^+_1 \otimes 2^+_1]_{\rm QRPA}$ configuration is the important component of the 1^+_2 wave function since the $[2^+_1]_{\rm QRPA}$ state is the lowest collective excitation which leads to the minimal two-phonon energy and the maximal matrix elements coupling one- and two-phonon configurations. The calculated energies and the $B(E2)$ values for up-transitions to the $[2^+_1]_{\rm QRPA}$ states of the parent nuclei ^{80}Zn and ^{82}Ge reproduce the experimental data very well [46]. The 2^+_1 state has a collective structure with the dominance of the proton configuration $\{1f_{5/2}, 1f_{5/2}\}$ whose contribution is about 53% (39%) for the case of ^{80}Zn (^{82}Ge). As a result, the inclusion of the four-quasiparticle configuration $\{\pi 2p_{3/2}\pi 1f_{5/2}\pi 1f_{5/2}\nu 2p_{1/2}\}$ plays a considerable role in the calculations of the $1^+_{1,2}$ states in ^{80}Ga and ^{82}As.

The spectrum of the calculated 1^+ states populated in the β decay of ^{80}Zn and ^{82}Ge is shown in Fig. 13. At a qualitative level, our results reproduce the experimental evolution of the spectrum, i.e., we describe the sharp reduction of the level density with increasing proton number from ^{80}Ga to ^{82}As. The influence of the coupling between one- and two-phonon terms in the 1^+ wave functions, as well as the tensor force effects, are the key mechanisms in question. When the tensor interaction is not included, the results within the one-phonon approximation indicate only three 1^+ states in ^{80}Ga and a β-stable ^{82}Ge [46].

For the calculated Q_β values of ^{80}Zn and ^{82}Ge (see Fig. 13), the quantitative agreement with the experimental data is not satisfactory. A possible reason might be the underestimated symmetry energy of 26.8 MeV in the case of the SGII effective

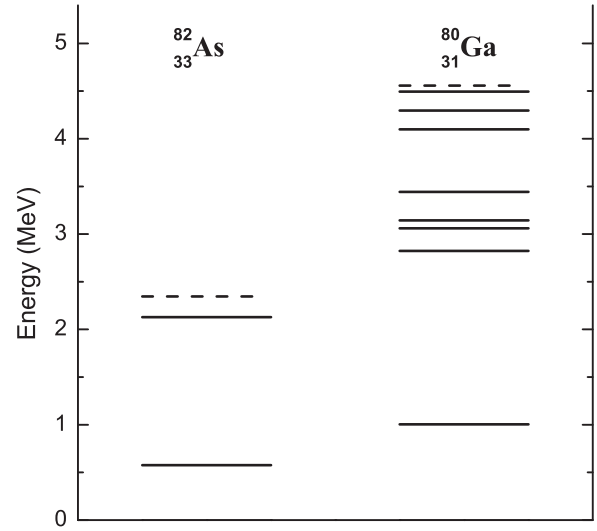

FIG. 13. Excitation energies of the 1^+ states calculated with the SGII+tensor force. The dashed lines correspond to the calculated energy of the Q_β window.

Skyrme interaction. Importantly, our model with the ansatz (2) enables one to study the spectroscopy of the odd-odd neutron-rich nuclei. Systematic calculations taking into account the tensor interaction for the different parametrizations of Skyrme effective interactions are now in progress.

V. SUMMARY AND CONCLUSION

The structure of ^{82}As has been investigated via β decay of a ^{82}Ge beam collected for the first time in the recently built BEDO decay station at ALTO. Data were collected taking advantage of the BEDO commissioning beam time. Notwithstanding the very short effective on-tape beam time and the complex composition of the beam, the quality of the data was sufficient to improve the level scheme with respect the only previous decay study available by the time of this experiment. Even with respect to the very recent concurrent work of [10] we were able to add three new transitions and two additional levels in the decay scheme, and our coincidence data appear somewhat richer. In addition, the decay curve measurements of 13 individual γ lines allow proposing a more precise determination of the ^{82}Ge half-life compared to what has been reported in the literature so far. These results, obtained with a still incomplete version of the detection array, offer a glimpse into the full potentialities of BEDO in its β-delayed γ-spectroscopy mode (details on the fast-timing and neutron-counting modes will be found in Refs. [20,22] respectively).

The two salient features revealed from our data are (i) several low-lying (below 1 MeV) low-spin states have a negative parity, in particular the state populated at 843 keV excitation energy for which $J = (0,1)$ and negative parity is almost certain; (ii) the extension of the ^{82}As level scheme towards higher energies from the present work has revealed only three potential additional 1^+ candidates above the already known one at 1092 keV.

Concerning point (i), it is clear that states with $J^\pi \leqslant 2^-$ (apart from the 2^- ground state) cannot find any counterparts in the natural valence space of ^{56}Ni. This is simply due to the fact that, in such restricted space, the lowest negative parity states can only be generated from the couplings of negative parity $\{f_{5/2}, p\}$ proton orbits to the high angular momentum positive parity neutron hole $g_{9/2}$. On the contrary, the occurrence of these states can easily be understood both on a qualitative level from careful zero-order coupling energy considerations and on a more quantitative level from core + 2QP calculations including $\{2d_{5/2}, 3s_{1/2}, 2d_{3/2}\}$ QP states located above the $N = 50$ shell gap. We show then clearly for the first time that the strong energy lowering of intruder states in $N = 49$ isotones at mid proton (28-40) shell, already hinted at in the case of odd nuclei a long time ago, dominates also the low-lying structure of the odd-odd nuclei. From that point of view it is clear now that attempts to describe the low-energy structure of light $N = 49$ isotones by shell model calculations will remain skewed unless neutron $\{2d_{5/2}, 3s_{1/2}, 2d_{3/2}\}$ orbitals are explicitly included in the valence space from the beginning.

Point (ii) above allows confirming that, in the odd-odd $N = 49$ isotone series towards ^{78}Cu, the occurrence of a large number of 1^+ states at low energy, directly populated in β decay, is of sudden character and appears between $Z = 33$ and $Z = 31$. This is consistent with the results of state-of-the-art Skyrme-QRPA calculations using the finite-rank separable approximation. In particular, the $\{\pi 2p_{3/2} \pi 1f_{5/2} \pi 1f_{5/2} \nu 2p_{1/2}\}$ configuration is the indispensable ingredient in the microscopic analysis of the $1^+_{1,2}$ states in ^{80}Ga and ^{82}As. These calculations provide an interpretation alternative to that of [9] concerning the large number of low-lying 1^+ states in ^{80}Ga. Important mechanisms which should be taken into account in these relatively weakly deformed nuclei are the coupling between one- and two-phonon terms in the 1^+ wave functions and the tensor force.

ACKNOWLEDGMENTS

The authors are most grateful to the Tandem/ALTO teams for their strong commitment into the BEDO project and the construction of the new secondary beam lines. We express our special thanks to A. Maroni, M. Imre, C. Thenau, B. Gajewski, B. Geoffroy, B. Mathon, L. Vatrinet, and M. Josselin from the R&D Detection Department of IPN for careful and skillful manufacturing, assembling, testing, and mounting of the various scintillation detectors of the BEDO assembly and their mechanical supports. The authors would also like to express their gratitude to Prof. G. Audi for illuminating discussions on the mass data network around ^{82}As. A.E. and D.V. would like to thank Dr. U. Köster for precious advice on the possible origin of the molecular beam composition and Dr. M. MacCormick for precious advice on the use of the NUBASE2012 evaluation. Use of Ge detectors from the French-UK IN2P3-STFC Gamma Loan Pool and from the EXOGAM Collaboration is acknowledged. P.V.C. acknowledges support from the bilateral agreement VAST-CNRS, the International Associated Laboratory (LIA) FV-PPL and Vietnam National Foundation for Science and Technology Development (NAFOSTED) under Grant No. 103.04-2014.29. A.G. was supported by the P2IO Excellence Laboratory. N.N.A, I.N.B, A.P.S., and V.V.V. thank the hospitality of IPN-Orsay where part of this work was done. This work is partly supported by the CNRS/IN2P3-JINR agreement. I.N.B. also acknowledges partial support of the National Research Center "Kurchatov Institute". Finally D.V. would like to acknowledge constant support from CNRS/IN2P3 to the BEDO project.

[1] P. Hoff and B. Fogelberg, Nucl. Phys. A **368**, 210 (1981).
[2] R. A. Meyer, O. G. Lien, and E. A. Henry, Phys. Rev. C **25**, 682 (1982).
[3] K. Heyde, P. V. Isacker, M. Waroquier, J. Wood, and R. Meyer, Phys. Rep. **102**, 291 (1983).
[4] K. Heyde and J. L. Wood, Rev. Mod. Phys. **83**, 1467 (2011).
[5] B. Ekstrom, B. Fogelberg, P. Hoff, E. Lund, and A. Sangariyavanish, Phys. Scr. **34**, 614 (1986).
[6] R. L. Gill, R. F. Casten, D. D. Warner, A. Piotrowski, H. Mach, J. C. Hill, F. K. Wohn, J. A. Winger, and R. Moreh, Phys. Rev. Lett. **56**, 1874 (1986).
[7] J. A. Winger, J. C. Hill, F. K. Wohn, R. Moreh, R. L. Gill, R. F. Casten, D. D. Warner, A. Piotrowski, and H. Mach, Phys. Rev. C **36**, 758 (1987).
[8] R. Lică, N. Mărginean, D. G. Ghiță, H. Mach, L. M. Fraile, G. S. Simpson, A. Aprahamian, C. Bernards, J. A. Briz, B. Bucher, C. J. Chiara, Z. Dlouhý, I. Gheorghe, P. Hoff, J. Jolie, U. Köster, W. Kurcewicz, R. Mărginean, B. Olaizola, V. Paziy, J. M. Régis, M. Rudigier, T. Sava, M. Stănoiu, L. Stroe, and W. B. Walters, Phys. Rev. C **90**, 014320 (2014).
[9] K.-L. Kratz, V. Harms, A. Wöhr, and P. Möller, Phys. Rev. C **38**, 278 (1988).
[10] K. Miernik, K. P. Rykaczewski, C. J. Gross, R. Grzywacz, M. Madurga, D. Miller, J. C. Batchelder, N. T. Brewer, C. U. Jost, K. Kolos, A. Korgul, C. Mazzocchi, A. J. Mendez, Y. Liu, S. V. Paulauskas, D. W. Stracener, J. A. Winger, M. Wolińska-Cichocka, and E. F. Zganjar, Phys. Rev. C **90**, 034311 (2014).
[11] F. Ajzenberg-Selove, E. R. Flynn, D. L. Hanson, and S. Orbesen, Phys. Rev. C **19**, 1742 (1979).
[12] F. Azaiez, S. Essabaa, F. Ibrahim, and D. Verney, Nucl. Phys. News **23**, 5 (2013).
[13] S. Essabaa, N. Barré-Boscher, M. C. Mhamed, E. Cottereau, S. Franchoo, F. Ibrahim, C. Lau, B. Roussière, A. Saïd, S. Tusseau-Nenez, and D. Verney, Nucl. Instrum. Methods B **317**, 218 (2013).
[14] J. K. Tuli, Nucl. Data Sheets **98**, 209 (2003).
[15] R. Kirchner, Nucl. Instrum. Methods B **204**, 179 (2003).
[16] U. Köster, O. Arndt, E. Bouquerel, V. Fedoseyev, H. Frånberg, A. Joinet, C. Jost, I. Kerkines, and R. Kirchner, Nucl. Instrum. Methods B **266**, 4229 (2008).
[17] O. Perru, F. Ibrahim, O. Bajeat, C. Bourgeois, F. Clapier, E. Cottereau, C. Donzaud, M. Ducourtieux, S. Galès, D. Guillemaud-Mueller, C. Lau, H. Lefort, F. Blanc, A. Mueller, J. Obert, N. Pauwels, J. Potier, F. Pougheon, J. Proust,

B. Roussière, J. Sauvage, O. Sorlin, and D. Verney, Phys. At. Nucl. **66**, 1421 (2003).
[18] K. Kolos, D. Verney, F. Ibrahim, F. Le Blanc, S. Franchoo, K. Sieja, F. Nowacki, C. Bonnin, M. Cheikh Mhamed, P. V. Cuong, F. Didierjean, G. Duchêne, S. Essabaa, G. Germogli, L. H. Khiem, C. Lau, I. Matea, M. Niikura, B. Roussière, I. Stefan, D. Testov, and J.-C. Thomas, Phys. Rev. C **88**, 047301 (2013).
[19] O. Perru, D. Verney, F. Ibrahim, O. Bajeat, C. Bourgeois, F. Clapier, E. Cottereau, C. Donzaud, S. Du, M. Ducourtieux, S. Essabaa, S. Galès, D. Guillemaud-Mueller, O. Hubert, C. Lau, H. Lefort, F. Le Blanc, A. Mueller, J. Obert, N. Pauwels, J. Potier, F. Pougheon, J. Proust, B. Roussière, J. Sauvage, and O. Sorlin, Eur. Phys. J. A **28**, 307 (2006).
[20] M. Cardona, D. Hojman, B. Roussière, I. Deloncle, N. Barré, M. Cheikh Mahmed, E. Cottereau, B. Dimitrov, G. Gavrilov, A. Gottardo, C. Lau, S. Roccia, S. Tusseau-Nenez, D. Verney, and M. Yavahchova (unpublished).
[21] D. Testov, Ph.D. thesis, Université Paris Sud, 2014 (unpublished).
[22] D. Testov, D. Verney, V. Smirnov, B. Roussière, J. Bettane, F. Didierjean, K. Flanagan, S. Franchoo, F. Ibrahim, E. Kuznetsova, R. Li, B. Marsh, I. Matea, Y. Penionzhkevich, E. Sokol, I. Stefan, and D. Suzuki (unpublished), http://www1.jinr.ru/Preprints/2014/085(E15-2014-85).pdf.
[23] M. Lebois, D. Verney, F. Ibrahim, S. Essabaa, F. Azaiez, M. Cheikh Mhamed, E. Cottereau, P. V. Cuong, M. Ferraton, K. Flanagan, S. Franchoo, D. Guillemaud-Mueller, F. Hammache, C. Lau, F. Le Blanc, J. F. Le Du, J. Libert, B. Mouginot, C. Petrache, B. Roussière, L. Sagui, N. de Séréville, I. Stefan, and B. Tastet, Phys. Rev. C **80**, 044308 (2009).
[24] L. A. Currie, Anal. Chem. **40**, 586 (1968).
[25] G. Gilmore and J. D. Hemingway, *Practical Gamma-Ray Spectrometry* (Wiley, New York, 1995).
[26] D. Symochko, S. Nafee, and J. Tuli, ENSDF (2011).
[27] H. Gausemel, K. A. Mezilev, B. Fogelberg, P. Hoff, H. Mach, and E. Ramström, Phys. Rev. C **70**, 037301 (2004).
[28] G. Audi, F. Kondev, M. Wang, B. Pfeiffer, X. Sun, J. Blachot, and M. MacCormick, Chin. Phys. C **36**, 1157 (2012).
[29] J. Hakala, S. Rahaman, V.-V. Elomaa, T. Eronen, U. Hager, A. Jokinen, A. Kankainen, I. D. Moore, H. Penttilä, S. Rinta-Antila, J. Rissanen, A. Saastamoinen, T. Sonoda, C. Weber, and J. Äystö, Phys. Rev. Lett. **101**, 052502 (2008).
[30] A. Pfeiffer, G. Mairle, K. Knöpfle, T. Kihm, G. Seegert, P. Grabmayr, G. Wagner, V. Bechtold, and L. Friedrich, Nucl. Phys. A **455**, 381 (1986).
[31] D. Verney, F. Ibrahim, C. Bourgeois, S. Essabaa, S. Galès, L. Gaudefroy, D. Guillemaud-Mueller, F. Hammache, C. Lau, F. L. Blanc, A. C. Mueller, O. Perru, F. Pougheon, B. Roussière, J. Sauvage, and O. Sorlin (PARRNe Collaboration), Phys. Rev. C **76**, 054312 (2007).
[32] M. Honma, T. Otsuka, T. Mizusaki, and M. Hjorth-Jensen, Phys. Rev. C **80**, 064323 (2009).
[33] K. Sieja and F. Nowacki, Phys. Rev. C **85**, 051301 (2012).
[34] J. Kitching, Z. Phys. **258**, 22 (1973).
[35] S. Bhattachrya and S. K. Basu, J. Phys. G: Nucl. Phys. **5**, 1163 (1979).
[36] P. H. Hoffmann-Pinther and J. L. Adams, Nucl. Phys. A **229**, 365 (1974).
[37] V. K. Thankappan and W. W. True, Phys. Rev. **137**, B793 (1965).
[38] J. W. Dawson, R. K. Sheline, and E. T. Jurney, Phys. Rev. **181**, 1618 (1969).
[39] B. Singh, Nucl. Data Sheets **94**, 1 (2001).
[40] P. H. Hoffmann-Pinther, Ph.D. thesis, Ohio University, 1973 (unpublished).
[41] A. P. Severyukhin, V. V. Voronov, and N. V. Giai, Prog. Theor. Phys. **128**, 489 (2012).
[42] A. P. Severyukhin and H. Sagawa, Prog. Theor. Exp. Phys. (2013) 103D03.
[43] N. Van Giai, C. Stoyanov, and V. V. Voronov, Phys. Rev. C **57**, 1204 (1998).
[44] V. G. Soloviev, *Theory of Atomic Nuclei: Quasiparticles and Phonons* (Institute of Physics, Bristol, 1992).
[45] V. A. Kuzmin and V. G. Soloviev, J. Phys. G **10**, 1507 (1984).
[46] A. P. Severyukhin, V. V. Voronov, I. N. Borzov, N. N. Arsenyev, and N. Van Giai, Phys. Rev. C **90**, 044320 (2014).
[47] J. Engel, M. Bender, J. Dobaczewski, W. Nazarewicz, and R. Surman, Phys. Rev. C **60**, 014302 (1999).
[48] A. P. Severyukhin, N. N. Arsenyev, and N. Pietralla, Phys. Rev. C **86**, 024311 (2012).
[49] N. V. Giai and H. Sagawa, Phys. Lett. B **106**, 379 (1981).
[50] C. L. Bai, H. Q. Zhang, X. Z. Zhang, F. R. Xu, H. Sagawa, and G. Colò, Phys. Rev. C **79**, 041301 (2009).
[51] G. Colò, H. Sagawa, S. Fracasso, and P. F. Bortignon, Phys. Lett. B **646**, 227 (2007); **668**, 457(E) (2008).